Deciphering locomotion in reptiles: application of elliptic Fourier transforms to femoral microanatomy

Jordan Gônet[1]* · Jérémie Bardin[1] · Marc Girondot[2] · John R. Hutchinson[3] · Michel Laurin[1]

[1]Centre de recherche en paléontologie – Paris, UMR 7207, Sorbonne Université, Muséum national d'histoire naturelle, Centre national de la recherche scientifique, 8 rue Buffon, 75005 Paris, France

[2]Laboratoire écologie, systématique et évolution, UMR 8079, AgroParisTech, Université Paris-Saclay, Centre national de la recherche scientifique, 91405 Orsay, France

[3]Structure and Motion Laboratory, Department of Comparative Biomedical Sciences, Royal Veterinary College, AL9 7TA Hatfield, UK

*Corresponding author: jordan.gonet@edu.mnhn.fr

Keywords: Adaptation · Comparative anatomy · Computed tomography · Discriminant-function analysis · Evolution · Fourier analysis · Functional morphology · Limb bones · Limb posture · Microstructure · Phylogenetics · Taxa

Abstract

Reptiles represent one of the most diverse groups of tetrapod vertebrates. Extant representatives of reptiles include lepidosaurs (lizards), testudines (turtles) and archosaurs (crocodiles and birds). In particular, they show an important locomotor diversity with bipedal, quadrupedal and facultatively bipedal taxa. This diversity is accompanied by substantial microanatomical disparity in the limb bones. Although many studies have highlighted the link between locomotion and bone microstructure, the latter has never been quantitatively studied from an angular perspective. Indeed, some taxa show microanatomical heterogeneity in cross-section. Here we show, using elliptic Fourier transforms and statistical analyses integrating phylogeny, how angular microanatomical parameters measured on reptilian femoral cross-sections, such as angular bone compactness, can be related to locomotion in this clade. Although phylogeny appears to have a significant impact on our results, we show that a functional signal exists. In particular, we show that bipeds and quadrupeds present a craniolateral-caudomedial and dorsoventral deficit in bone compactness, respectively. This reflects cross-sectional eccentricity in these directions that we relate to the forces acting upon the femur in different postural contexts. This work contributes to deciphering the complex interplay between phylogeny, femoral cross-sectional microanatomy and locomotion in reptiles.

Introduction

Reptiles are a remarkably successful group of tetrapod vertebrates originating in the Carboniferous, about 330 Mya (Didier & Laurin, 2020) that experienced several episodes of diversification throughout their evolutionary history (Sues, 2019). The oldest known reptile, *Hylonomus lyelli* (Dawson, 1860), lived between 315–320 Mya in what is now Nova Scotia, Canada (Utting *et al.*, 2010; Rygel *et al.*, 2015); however, the Mesozoic is recognised as the 'golden age' of reptiles, with dinosaurs roaming the Earth for nearly 200 Myr.

In the traditional Linnean classification system, the term 'reptile' refers to 'cold-blooded' (ectothermic) tetrapods with scaly skin. With the advent of cladistics, it became evident that reptiles (Reptilia), as defined above, were paraphyletic. Indeed, after being heatedly debated for over a century, in line with the discovery of *Archaeopteryx* (von Meyer, 1861), the dinosaurian origin of birds is now consensual (Huxley, 1868; Fürbringer, 1888; Simpson, 1946; Ostrom, 1969, 1975; Bakker & Galton, 1974; Sereno, 1997; Padian & Chiappe, 1998; Dodson, 2000; Benton *et al.*, 2019). Birds are therefore dinosaurs and, together with Crocodylia, they form the clade Archosauria, within Reptilia. Extant representatives of reptiles include lepidosaurs, turtles, crocodylians and birds. They are incredibly diverse in terms of morphology, physiology and lifestyle (Pianka & Vitt, 2003; Wyneken *et al.*, 2007; Brett-Surman *et al.*, 2012; Grigg & Kirshner, 2015; Lovette & Fitzpatrick, 2016). In particular, they exhibit a great variety of modes of locomotion and postures: birds are erect bipeds; crocodylians are sometimes classified as 'semi-erect' quadrupeds; most lepidosaurs are sprawling quadrupeds, but some are able to become bipeds while running (facultative bipedalism); and turtles are sprawling quadrupeds (Gatesy, 1991; Reilly & Elias, 1998; Blob & Biewener, 2001; Hutchinson & Gatesy, 2001; Clemente & Wu, 2018; Nyakatura *et al.*, 2019).

This locomotor and postural diversity is accompanied by important microanatomical disparity. Indeed, bone is a living tissue that is constantly undergoing modelling and remodelling (changing shape to maintain strength and repair micro-damage, respectively) under the action of osteoblasts and osteoclasts that participate in the formation and destruction of this tissue, respectively (Currey, 2013). This process is driven by fine molecular control, but also by mechanical regulation to maintain or increase bone strength (Robling *et al.*, 2006). The bones of the appendicular skeleton, in particular, bear the weight of the body and are constrained by forces that partly shape their external and internal morphology. Many studies have already identified the link between lifestyle (aquatic to terrestrial) and bone microanatomy (Germain &

Laurin, 2005; Kriloff *et al.*, 2008; Canoville & Laurin, 2009, 2010; Laurin *et al.*, 2011; Quemeneur *et al.*, 2013; Amson *et al.*, 2014; Ibrahim *et al.*, 2014; Nakajima *et al.*, 2014; Cooper *et al.*, 2016; Houssaye *et al.*, 2016a; Klein *et al.*, 2016; Houssaye & Botton-Divet, 2018; Fabbri *et al.*, 2022), and also between locomotion/ posture and microanatomy (Houssaye *et al.*, 2016b; Bishop *et al.*, 2018a, b, c; Plasse *et al.*, 2019; Wagstaffe *et al.*, 2022). However, few have attempted to characterise microanatomy in an angular fashion; i.e. how the microanatomy of long bones varies with anatomical direction of the limb (anteroposterior/mediolateral). Dumont *et al.* (2013) analysed angular parameters of microanatomy on vertebral centra of terrestrial and aquatic mammals, but to our knowledge nothing like this has been studied on reptile femoral cross-sections.

Fourier decomposition/transformation, named after its author, the French mathematician Joseph Fourier, is a mathematical procedure consisting of reducing a complex general function into a sum of simpler functions, called harmonics, in order to facilitate its study. Each harmonic is described by several coefficients. Today, Fourier analysis is extensively used in various scientific fields such as physics (Ransom *et al.*, 2002) and engineering (Cadet *et al.*, 2018), but also biology and palaeontology, especially for the study of biological shapes in morphometric studies (Bonhomme *et al.*, 2013; Caillon *et al.*, 2018; Kruta *et al.*, 2020; Zaharias *et al.*, 2020).

In this article, we use elliptic Fourier transforms to study the angular variation of several microanatomical parameters measured on mid-diaphyseal transverse sections of reptile femora with the BONEPROFILER software (Girondot & Laurin, 2003; Gônet *et al.*, 2022), such as bone compactness and the distance from the centre of the cross-section of the medullocortical transition, in order to quantitatively test for the first time if there is a relationship between locomotion and angular microanatomy in reptiles. We hypothesise that angular bone compactness varies according to the different mechanical constraints experienced by the femur of reptiles using different modes of locomotion. We also use statistical methods that take phylogeny into account, to study the impact of different factors such as body mass and functional ecology on the microanatomical parameters.

Materials and Methods

BIOLOGICAL SAMPLE

We collected angular microanatomical data from mid-diaphyseal cross-sections of femora belonging to a large number of adult extant reptiles, i.e. 47 specimens from 45 taxa, including

31 archosaur, 12 lepidosaur and two turtle taxa (Fig. 1; Table 1; Supporting Information, Table S1). In order to expand the size range of bipeds, but also to provide temporal depth to our sample, we included six extinct theropod taxa (three non-avian, three avian), which were all fully bipedal (Hutchinson & Gatesy, 2001): the Mesozoic species *Allosaurus fragilis* (Marsh, 1877), *Masiakasaurus knopfleri* (Sampson *et al.*, 2001) and *Tyrannosaurus rex* (Osborn, 1905), and the Quaternary species *Dinornis* sp. (Owen, 1843), *Pezophaps solitaria* (Gmelin, 1789) and *Raphus cucullatus* (Linnaeus, 1758).

LOCOMOTION

Reptiles exhibit a wide range of locomotor habits. Bipedalism in our sample is exclusive to theropods (Hutchinson & Gatesy, 2001). Quadrupedalism occurs in most lepidosaurs and all turtles and crocodylians (Bels & Russell, 2019). For these examples, bipedalism and quadrupedalism are strict and are functionally imposed insofar as it is impossible for a bird to stand on four limbs (it can technically push on the ground with its wings, but this is not considered locomotion) or for the majority of lepidosaurs to adopt bipedal locomotion, especially for standing or slow walking. Some varanids may adopt a tripodal stance during intraspecific fights, standing on their hind limbs with their tail touching the ground (Schuett *et al.*, 2009), but this is not bipedalism because it corresponds to brief moments that involve little movement. Nevertheless, bipedalism and quadrupedalism do not correspond to compartmentalised functional categories. Indeed, some lepidosaurs spontaneously alternate between bipedalism and quadrupedalism. *Basiliscus basiliscus* (Linnaeus, 1758), the common basilisk, and *Chlamydosaurus kingii* (Gray, 1825), the frilled dragon, are some examples (Bennett, 1875; Snyder, 1949). In these reptiles, bipedalism is usually associated with running (Bels & Russell, 2019) and they spend a considerable amount of time on all fours. This is called facultative bipedalism (Hutchinson & Gatesy, 2001; Demes, 2011; Grinham & Norman, 2020). The locomotor habit for each taxon in this study is reported in Table 1 and in the Supporting Information (Table S1).

FUNCTIONAL ECOLOGY AND BODY MASS ESTIMATES

To explore the potential relationship between lifestyle and microanatomy, we defined four functional ecology categories based on limb use (Bels & Russell, 2019): semi-aquatic, terrestrial, fossorial and arboreal.

We collected body mass estimates from the literature for each taxon in our sample to investigate a possible association between body mass and microanatomical parameters. We

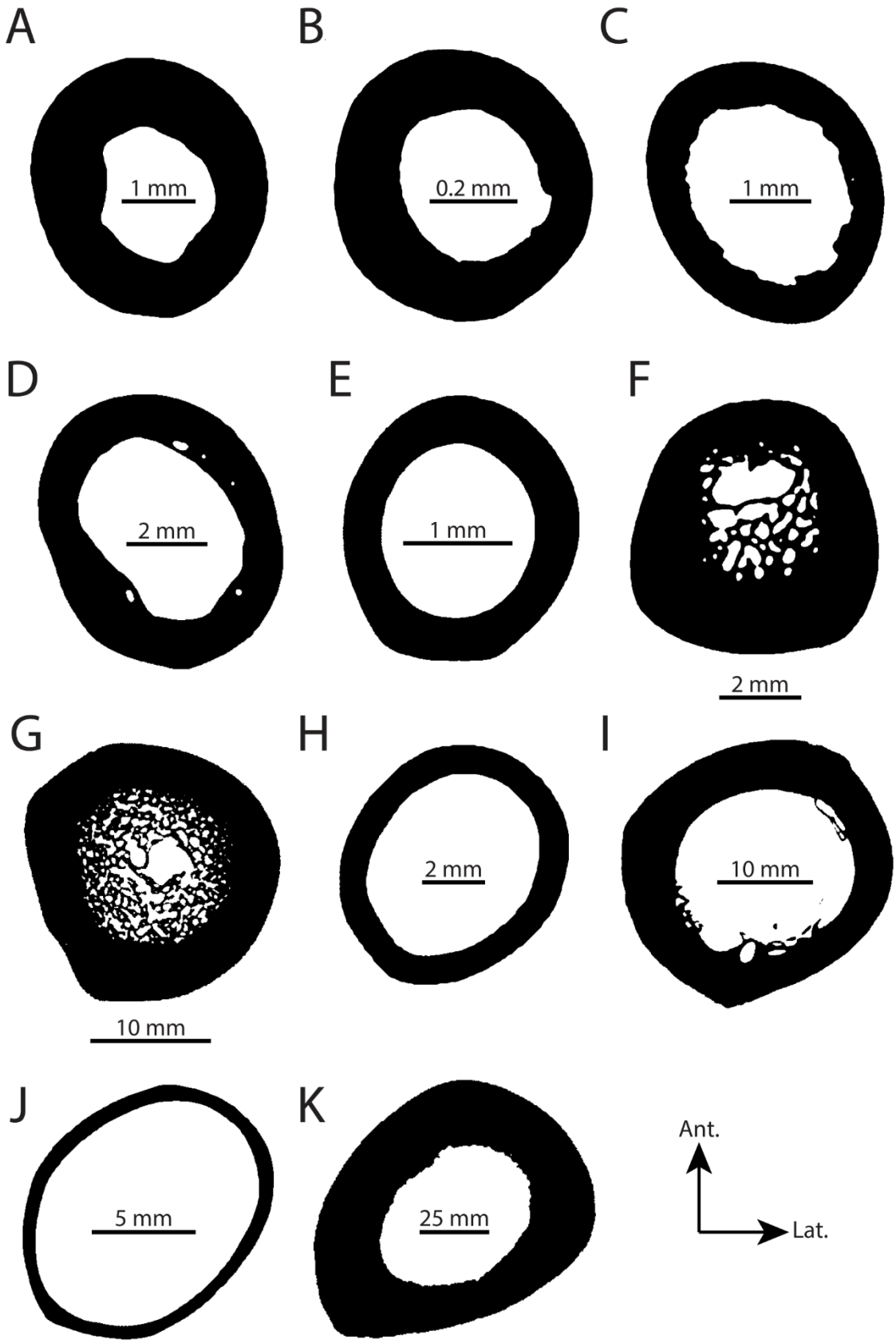

Figure 1. Some of the femoral cross-sections used in this study. A, *Sphenodon punctatus*, ummz:herps:40651 (sprawling quadruped); B, *Urosaurus bicarinatus*, unnumbered specimen (sprawling quadruped); C, *Varanus gouldii*, MNHN-ZA-AC-1889-62 (sprawling quadruped);

D, *Cyclura cornuta*, MNHN-ZA-AC-1907-107 (sprawling quadruped); E, *Basiliscus vittatus*, MNHN-ZA-AC-1883-1830 (sprawling facultative biped); F, *Chelonoidis carbonaria*, MNHN-ZA-AC-1877-404 (sprawling quadruped); G, *Alligator mississippiensis*, MNHN-ZA-AC-1945-54 ('semi-erect' quadruped); H, *Phasianus colchicus*, YPM 7778 (crouched biped); I, *Casuarius casuarius*, MNHN-ZO-AC-1946-72 (erect biped); J, *Sagittarius serpentarius*, YPM 1797 (crouched biped); K, *Allosaurus fragilis* (Tithonian), DNM 2560 (erect biped).

relied primarily on the database of Myhrvold *et al.* (2015), which contains median masses for a large number of extant amniotes. When only the genus was known, the mean median body mass of the relevant genus was used. We used the cQE function from the R package MASSTIMATE (Campione, 2020) to estimate body mass for the bipedal non-avian theropods in our sample from femur circumference (Campione & Evans, 2012; Campione *et al.*, 2014). Based on femoral circumference, body mass in MOR 1125 ('B-rex') is estimated at approximately 9.5 t. This result is close to or exceeds the highest estimates associated with the largest *Tyrannosaurus rex* individuals, i.e. FMNH PR 2081 ('Sue') and RSM P2523.8 ('Scotty'): 9.5 t and 8.87 t, respectively (Hutchinson *et al.*, 2011; Persons *et al.*, 2020). However, on the basis of femoral length, MOR 1125 is smaller than the aforementioned *T. rex* individuals. This leads us to believe that our methodology overestimated body mass in MOR 1125. This is most likely because we could not obtain a cross-section where the diaphyseal perimeter was smallest due to poor scan contrast. Therefore, we relied on the literature for this taxon (Hutchinson *et al.*, 2011; Campione *et al.*, 2014). Because the range of body mass in our sample is large (from 3 g to 7000 kg; see Table 1), we applied a $\log_{10}$ transformation to body mass.

Assignment to a functional ecology category and body mass estimates for each of the studied taxa are presented in Table 1. The associated literature is available in the Supporting Information (Table S1).

BONE ORIENTATION AND DATA ACQUISITION

We measured different microanatomical parameters of femoral diaphyseal cross-sections obtained mainly via computed tomography (CT) scan data retrieved from the literature and from morphosource.org. We scanned some specimens on the tomography platforms of the Muséum national d'histoire naturelle (MNHN), Paris and the Université de Montpellier. We extracted cross-sections from the CT scan data where the diaphysis had the smallest perimeter. Traditional histological sections were also incorporated into our database. For histological sect-

166 **Table 1.** List of the femora from adult extant and extinct (†) reptiles used in this study

Taxon		Collection number	Locomotor mode	Functional ecology	Body mass (g)	Femoral cross-section	CT resolution (µm)
Accipitridae	*Gypaetus barbatus*	MNHN-ZO-AC-1993-52	B	Te	5606.042	CT scan	30
Anatidae	*Anas superciliosa*	UMZC 222.a	B	Aq	981	CT scan	31
	Anser albifrons	UMZC 242.e	B	Aq	2387.5	CT scan	37
	Branta bernicla	UMZC 246.f	B	Aq	1347.25	CT scan	36
	Cereopsis novaehollandiae	UMZC 242.aa	B	Aq	3770	CT scan	51
	Chenonetta jubata	UMZC 246.g	B	Aq	812.5	CT scan	29
	Cygnus olor	RVC	B	Aq	10230	CT scan	60
	Somateria mollissima	UMZC 704	B	Aq	2092	CT scan	36
Alligatoridae	*Alligator mississippiensis*	MNHN-ZA-AC-1945-54	Q	Aq	62000	CT scan	46
	Caiman crocodilus	MNHN-ZA-AC-1910-87	Q	Aq	10900	CT scan	30
Allosauridae†	*Allosaurus fragilis†*	DNM 2560	B	Te	1820150	CT scan	549
Apterygidae	*Apteryx australis*	UMZC 378.s	B	Te	2600	CT scan	61
	Apteryx haastii	UMZC 378.p	B	Te	2409	CT scan	44
	Apteryx owenii	UMZC 378.iii	B	Te	1200	CT scan	46
Casuariidae	*Casuarius casuarius*	MNHN-ZO-AC-1946-72	B	Te	44000	CT scan	57
	Dromaius novaehollandiae	YPM 2128	B	Te	36200	CT scan	186
Columbidae	*Columba livia*	RVC	B	Te	320	CT scan	25
	Pezophaps solitaria†	YPM 1154	B	Te	14000	CT scan	19
	Raphus cucullatus†	YPM 2064	B	Te	14000	CT scan	19
Crocodylidae	*Crocodylus niloticus*	MNHN-ZA-AC-1963-22	Q	Aq	94200	CT scan	57
Cuculidae	*Geococcyx californianus*	UMZC 429.p	B	Te	376	CT scan	32
Dinornithidae†	*Dinornis* sp.†	YPM 421	B	Te	173500	CT scan	285
Megapodiidae	*Alectura lathami*	YPM 379	B	Te	2330	CT scan	188
Noasauridae†	*Masiakasaurus knopfleri†*	FMNH PR 2117	B	Te	18 849.1	CT scan	188
Numididae	*Numida meleagris*	RVC	B	Te	1375	CT scan	55
Phasianidae	*Afropavo congensis*	YPM 6658	B	Te	1149.25	CT scan	188

	Argusianus argus	YPM 2100	B	Te	2280.5	CT scan	188
	Synoicus ypsilophorus	UMZC 405.a	B	Te	107.5	CT scan	5
	Dendragapus obscurus	YPM 11600	B	Te	1059	CT scan	188
	Gallus sp.	RVC	B	Te	828.9	CT scan	37
	Meleagris gallopavo	RVC	B	Te	5811	CT scan	72
	Phasianus colchicus	YPM 7778	B	Te	1043.75	CT scan	188
Rheidae	*Rhea americana*	MNHN-ZO-AC-1876-730	B	Te	23000	CT scan	57
Sagittariidae	*Sagittarius serpentarius*	YPM 1797	B	Te	3900	CT scan	188
Struthionidae	*Struthio camelus*	RVC	B	Te	109250	CT scan	390
Tinamidae	*Eudromia elegans*	MNHN-ZO-AC-1905-31	B	Te	678	CT scan	24
	Eudromia elegans	UMZC 404.e	B	Te	678	CT scan	188
Tyrannosauridae†	*Tyrannosaurus rex†*	MOR 1125	B	Te	7000000	CT scan	1178
Sphenodontidae	*Sphenodon punctatus*	uf:herp:14110*	Q	Fo	430	CT scan	74
	Sphenodon punctatus	ummz:herps:40651*	Q	Fo	430	CT scan	105
Agamidae	*Chlamydosaurus kingii*	ypm:vz:ypm herr 010336*	FB	Ar	449.125	CT scan	127
Corytophanidae	*Basiliscus basiliscus*	MNHN-ZA-AC-1888-124	FB	Ar	225	CT scan	15
	Basiliscus vittatus	MNHN-ZA-AC-1883-1830	FB	Ar	60.87	CT scan	15
Eublepharidae	*Coleonyx elegans*	ummz:herps:125878*	Q	Te	11.2	CT scan	56
Iguanidae	*Cyclura cornuta*	MNHN-ZA-AC-1907-107	Q	Te	16 578.115	CT scan	34
	Iguana iguana	MNHN-ZA-AC-1974-129	Q	Ar	1530	CT scan	34
Phrynosomatidae	*Phrynosoma cornutum*	MNHN-ZA-AC-1893-662	Q	Te	27.335	CT scan	11
	Urosaurus bicarinatus	Unnumbered specimen	Q	Ar	3.415	Histological section	
Scincidae	*Tiliqua scincoides*	MNHN-ZA-AC-1898-285	Q	Te	496.4	CT scan	15
Varanidae	*Varanus gouldii*	MNHN-ZA-AC-1889-62	Q	Fo	671.92	CT scan	15
	Varanus griseus	MNHN-ZA-AC-1920-146	Q	Fo	821.1	Histological section	
Chelydridae	*Chelydra serpentina*	MNHN-ZA-AC-1897-255	Q	Aq	5170	CT scan	24
Testudinidae	*Chelonoidis carbonarius*	MNHN-ZA-AC-1877-404	Q	Te	2000	CT scan	30

*Data collected from https://www.morphosource.org. Abbreviations: Aq, semi-aquatic; Ar, arboreal; B, biped; FB, facultative biped; Fo, fossorial; Q, quadruped; Te, terrestrial. Daggers indicate extinct taxa.

ions, the reference plane was located at mid-shaft. Mixing sections from different diaphyseal locations in a comparative framework is not a problem as long as the taxa in question do not show excessive longitudinal microanatomical variation (Amson & Kolb, 2016; Houssaye *et al.*, 2018). Here, the taxa for which we used histological cross-sections, i.e. *Urosaurus bicarinatus* (Duméril, 1856) and *Varanus gouldii* (Gray, 1838), both present a tubular shaft. Scans were processed in IMAGEJ v. 1.51h (Abràmoff *et al.*, 2004) and MORPHODIG v. 1.5.3 (Lebrun, 2018). Each bone was oriented so that the section plane was as perpendicular as possible to the axis of the diaphysis. As we wanted to study microanatomical angular variations, we used the intercondylar fossa to determine the anterior aspect of the femur (Fig. 2). All left femora were mirrored to study only right femora. Some scans were of modest quality, so we increased the resolution using bicubic interpolation in IMAGEJ. Finally, we binarised the cross-sections before taking our microanatomical measurements with BONEPROFILER v. 2.0-7 (Girondot & Laurin, 2003; Gônet *et al.*, 2022).

MICROANATOMICAL MEASUREMENTS

BONEPROFILER is a computer program that extracts different microanatomical parameters from a compactness profile. We provide here a brief summary of how BONEPROFILER works; see Gônet *et al.* (2022) for a detailed description of its functioning. BONEPROFILER segments a bone cross-section into concentric circles (100 by default). Here, we decided to use the centre of the medullary cavity, i.e. the centre of unmineralised spaces in the bone section. The observed bone compactness (the number of bone pixels; C_{obs}) is measured in each circle starting with the smallest (near the centre). C_{obs} varies between 0 and 1; 0 signifies null compactness (typically, at the centre of the section) and 1 signifies maximum compactness (typically at the edge of the section). A sigmoid curve is then modelled from these measurements: this is the compactness profile (Fig. 3). Several parameters can be extracted from this profile: Min and Max represent respectively the asymptotic minimum and maximum compactness; P corresponds to the point of inflection of the sigmoid curve, it represents the distance from the centre of the cross-section to the transition between the medullary cavity (the void) and the cortex (the bone); and S is the inverse of the tangent to the modelled curve at point P, it gives information on the extension of this transition. BONEPROFILER also offers the possibility to perform angular measurements: the section is segmented into equal slices (here, 60 slices of 6°) and a compactness profile is drawn for each of them.

We were particularly interested in how the medullocortical transition varies depending on the position on the slice. We therefore used the measures of C_{obs}, P and S, which in our case

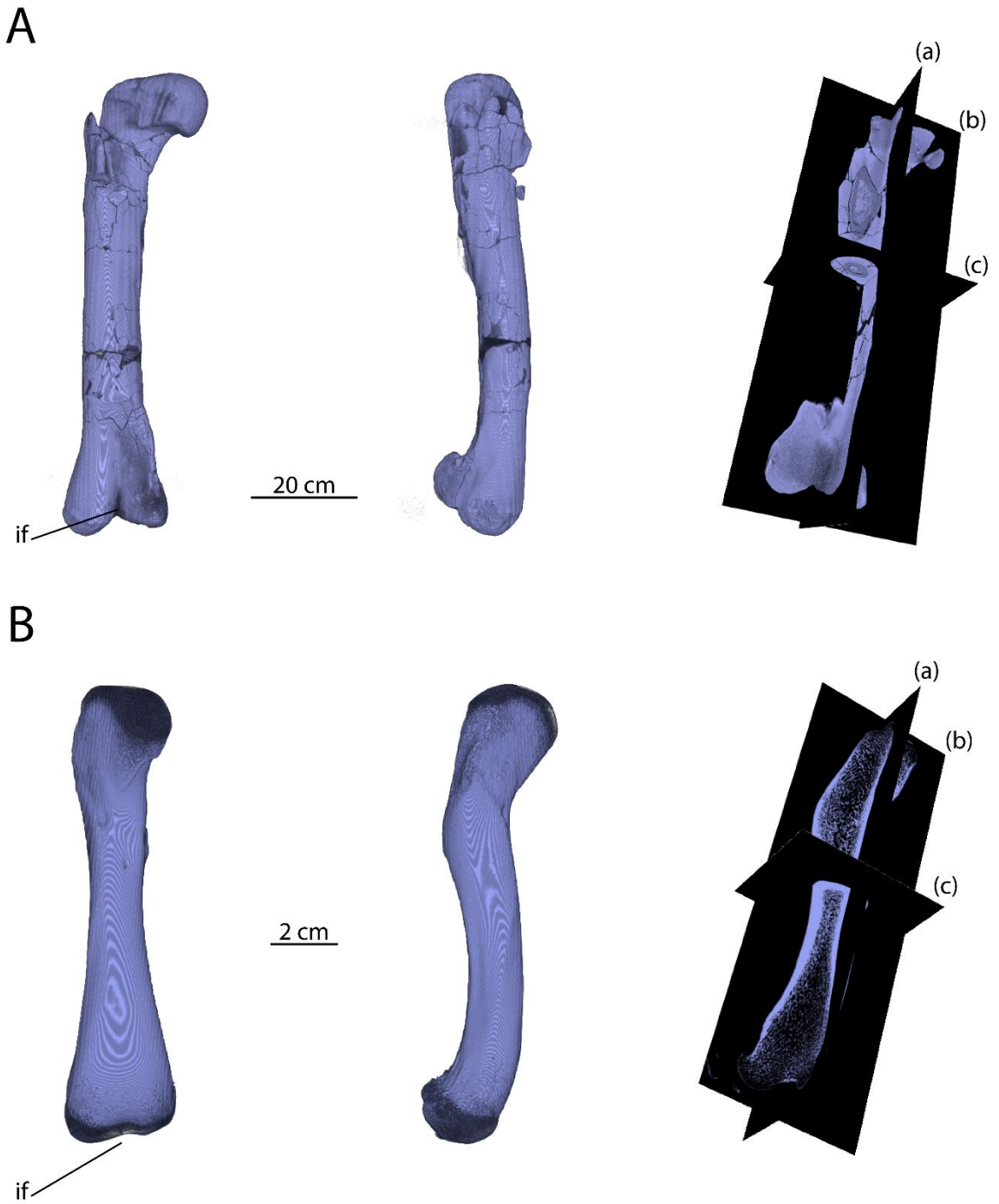

Figure 2. Orientation of the studied femora in the traditional anatomical system. A, mirrored *Allosaurus fragilis* (DNM 2560) femur and B, mirrored *Alligator mississippiensis* (MNHN-ZA-AC-1945-54) femur in anterior (left), lateral (centre) and orthogonal (right) views. We oriented the femora so that the intercondylar fossa (if) faced forward. Orthogonal planes: anteroposterior plane (a); mediolateral plane (b); cross-sectional plane (c).

are the most important parameters to characterise this transition (Min and Max representing only extreme values), from each of the slices and calculated the associated standard deviations (C_{obs}.SD, P.SD and S.SD). For the S.SD parameter, values were $\log_{10}$ transformed due to the

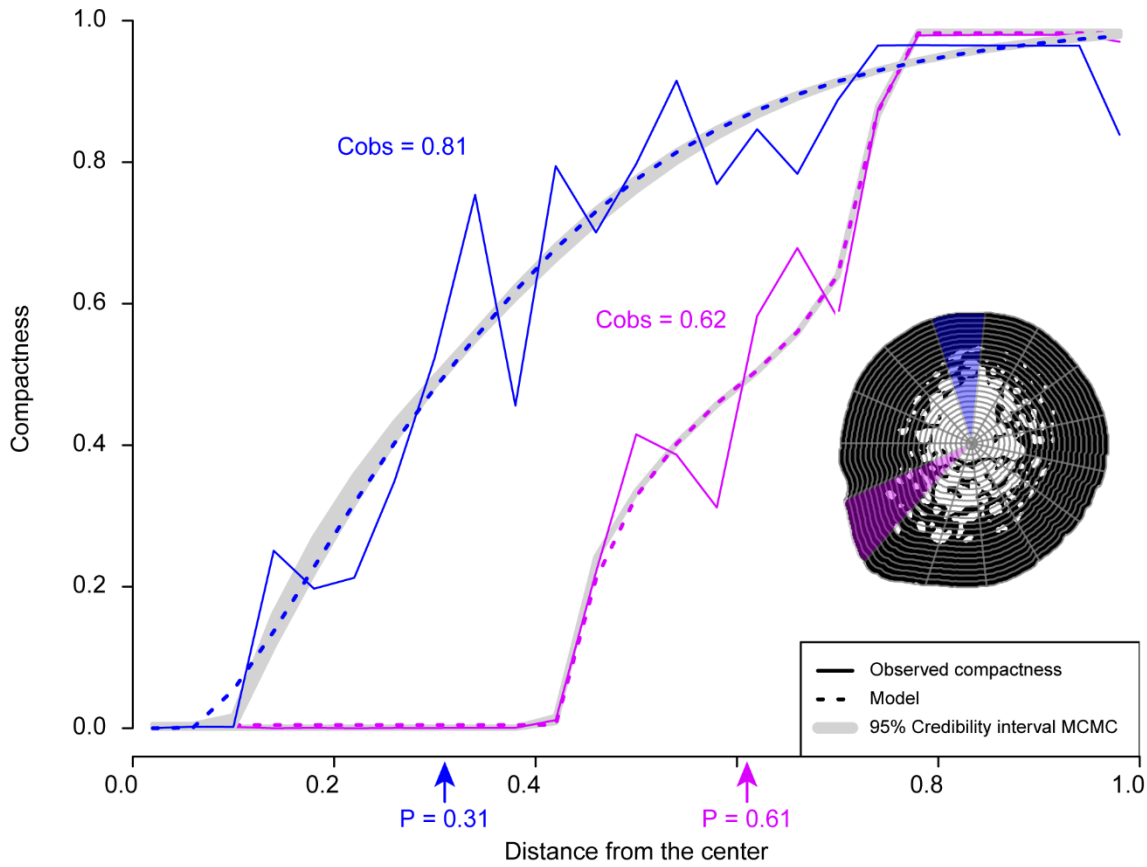

Figure 3. Compactness profiles for two slices of a mid-diaphyseal femoral cross-section of *Chelydra sepentina* (MNHN-ZA-AC-1897-255) showing variations of the medullocortical transition obtained with BONEPROFILER (Gônet et al., 2022). An observed global compactness (C_{obs}) is calculated for each slice. The parameters P and S are extracted from the modelled curve: P, the distance from the centre of the medullocortical transition; and S, the inverse of the tangent to the curve at point P (0.14 and 0.22 for the blue and purple slices, respectively).

wide dispersion of the data. For taxa represented by several individuals, we calculated the mean value for each parameter.

ELLIPTIC FOURIER AND PRINCIPAL COMPONENT ANALYSES

We applied elliptic Fourier transforms (Kuhl & Giardina, 1982) to the angular measurements of C_{obs}, P and S to study the variability of the medullocortical transition depending on its position in the anatomically oriented cross-sectional plane. This was done with the efourier function of the R package Momocs (Bonhomme *et al.*, 2014). For the angular analysis of a given microanatomical parameter, BONEPROFILER generates two vectors (one containing the slice positions in radians, and the other containing the microanatomical measurements). As the

efourier function was designed for shapes, we projected the microanatomical measurements (60 per cross-section) into a two-dimensional space with xy coordinates (Fig. 4), before embedding them into a collection of coordinates (COO) object recognised by the function. The analysis returns a collection of coefficients (COE) object with the harmonic coefficients for each of the cross-sections. We prevented the normalisation of the coefficients by setting the norm argument to 'FALSE'. Indeed, by default, the function normalises the shapes in terms of size and rotation based on the 'first ellipse', i.e. the coefficients of the first harmonic. Instead, we pre-aligned the shapes based on the positional homology between the taxa (Fig. 2). We used the calibrate_harmonicpower_efourier function to determine the optimal number of harmonics to include in the analysis. The cumulative power of the harmonics may be considered a measure of the amount of contour information carried by these harmonics (Bonhomme *et al.*, 2014). We selected the number of harmonics that represent 95% of the cumulative harmonic power. We then performed a principal component analysis (PCA) on the Fourier coefficients.

STATISTICAL TREATMENT IN A PHYLOGENETIC CONTEXT

Building a set of reference time-calibrated phylogenies

Most statistical analyses require the data to be independent, which is not the case when observations are made on evolutionarily related taxa. Indeed, many observable traits are the result of a shared evolutionary history between taxa, and it is necessary to take this fact into account in order to minimize interpretation bias (Felsenstein, 1985; Martins & Hansen, 1997). To this end, we built a set of 100 time-calibrated phylogenetic trees of reptiles (Fig. 5). These are composite trees since, to our knowledge, there is no published phylogeny that includes all the sampled taxa. A detailed explanation of the procedure we followed to assemble the trees is presented in the Supporting Information File S1, as well as the trees in Newick format (Supporting Information, File S2).

Phylogenetic signal

We used the phylosig function from the R package phytools (Revell, 2012; R Core Team, 2013) to calculate the K-statistic of Blomberg *et al.* (2003), which is designed to estimate the phylogenetic signal in continuous data. The latter is compared to the signal expected under a Brownian model of evolution (K = 1). A K-statistic greater than 1 suggests that closely related species in the tree are more similar to each other than would be expected with a Brownian model of evolution, implying a substantial phylogenetic signal in the data. Conversely, a K-statistic below 1 suggests that closely related species are less similar than expected, implying a pattern

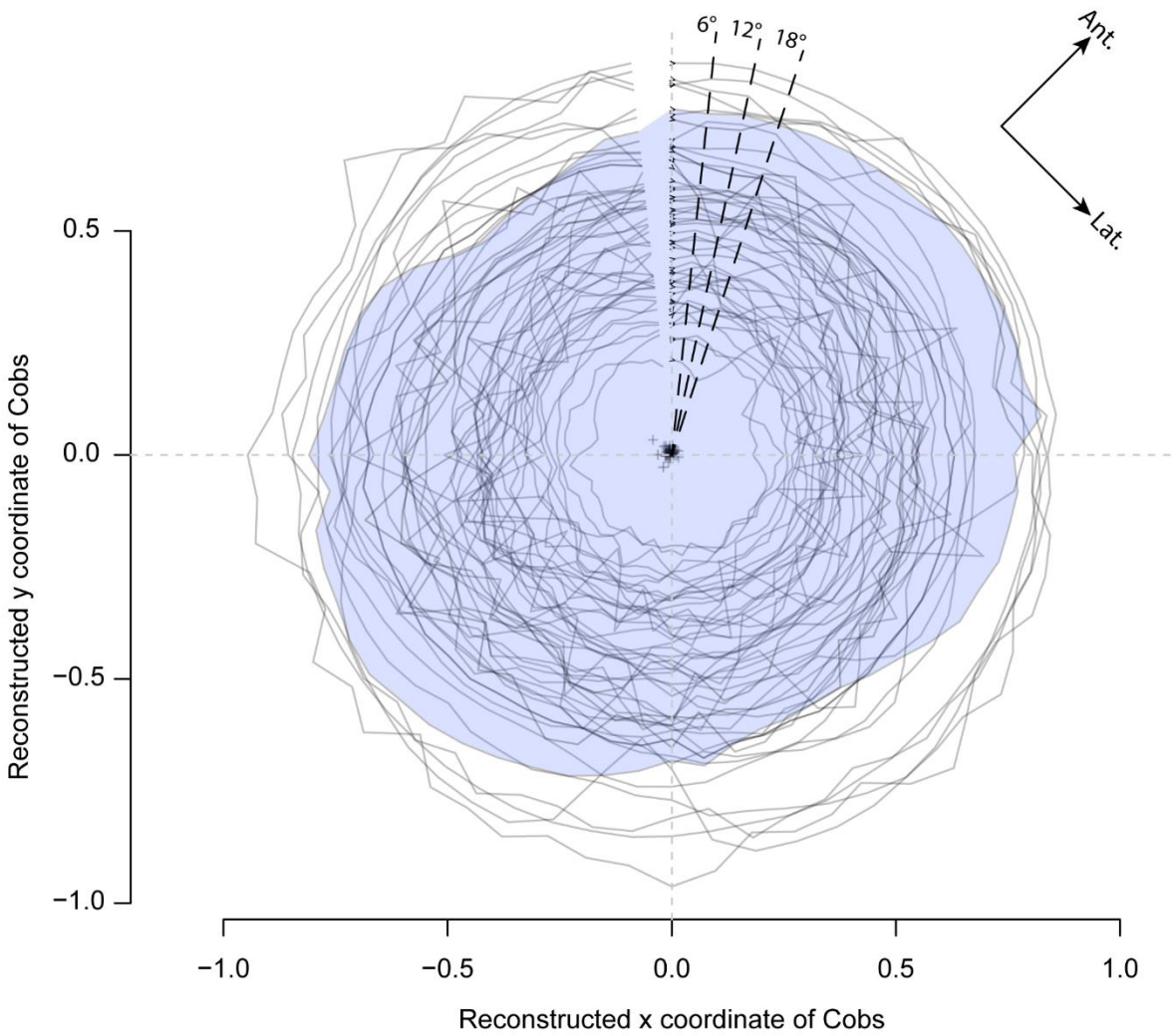

Figure 4. Xy projection stacks of angular C_{obs} values for the 51 reptile taxa in this study. C_{obs}, and the other microanatomical parameters, P and S, are measured in 6° increments with BONEPROFILER (Gônet *et al.*, 2022). The purple region corresponds to C_{obs} measurements for *Tiliqua scincoides* (MNHN-ZA-AC-1898-285).

of evolutionary convergence or a higher variance among rather than within clades. The phylosig function also provides a way to compute a *P*-value using a randomisation process. We searched for a phylogenetic signal in body mass and in the microanatomical parameters C_{obs}.SD, P.SD and S.SD with our 100 phylogenetic trees.

For locomotion, we used the delta-statistic (Borges *et al.*, 2019), which was designed to evaluate the phylogenetic signal in discrete data. The more a trait follows the phylogeny, the less uncertainty there is in the reconstruction of ancestral states. The delta value is based on this uncertainty: the lesser the uncertainty, the stronger the phylogenetic signal, and the higher the delta-statistic. A *P*-value is obtained by a randomisation process. We calculated a delta-statistic and its associated *P*-value for each of our 100 phylogenetic trees.

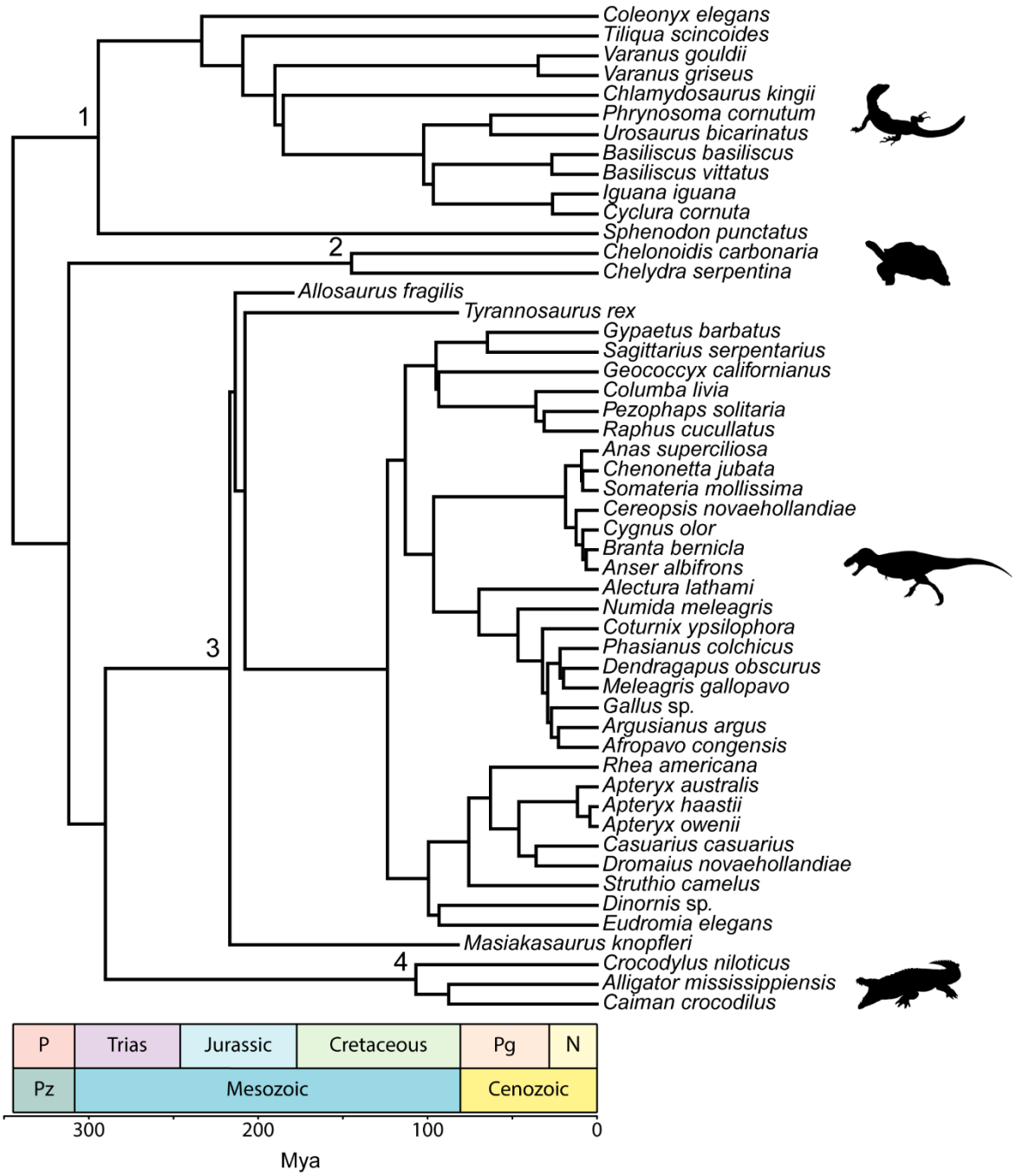

Figure 5. Tree 1 of our set of 100 time-calibrated composite phylogenies displaying the evolutionary relationships among the 51 reptile taxa in this study. Trees were compiled in R using the work of Shapiro et al. (2002), Chiari et al. (2012), Jetz et al. (2012), Joyce et al. (2013), Bapst et al. (2016), Tonini et al. (2016), Turner et al. (2017), Rauhut & Pol (2019) and Drumheller & Wilberg (2020). 1, Lepidosauria; 2, Testudines; 3, Dinosauria; 4, Crocodylia. Taxon silhouettes are taken from PhyloPic.

Phylomorphospaces

Using the R package phytools (Revell, 2012), we plotted a phylogenetic tree on the PCA graphs to visualise the spread of the different clades, and thus attempt to reveal a possible impact of the phylogeny.

Impact of body mass

We used phylogenetic generalised least squares (PGLS) in R to study the association of body mass with the different microanatomical parameters and with the coordinates of each taxon on the first PC of the Fourier-derived PCAs. We performed PGLS using the caper package (Orme *et al.*, 2018). PGLS fits a linear regression between a dependent variable and one or more independent variables while accounting for relatedness between taxa (Symonds & Blomberg, 2014). This is done by adjusting branch length transformations with the optimal lambda parameter (Pagel, 1999) obtained by maximum likelihood. PGLS were performed with 100 phylogenetic trees.

Influence of locomotion and functional ecology

We used the phylogenetic analysis of variance (ANOVA) of Garland *et al.* (1993) implemented by the phylANOVA function in the R package phytools (Revell, 2012) to investigate the impact of locomotion and functional ecology on microanatomical parameters (when a parameter was significantly associated with body mass, we used the residuals from the PGLS model instead of the original values) and on the coordinates of each taxon on the first PC of the Fourier-derived PCAs. Significant ANOVAs were followed by pairwise post-hoc tests with false discovery rate (FDR) correction to explore differences between group means while controlling for experimental error rate. Phylogenetic ANOVAs were performed with 100 phylogenetic trees.

Phylogenetic flexible discriminant analyses

We used phylogenetic flexible discriminant analysis (PFDA) to explain locomotion from the first PC of the Fourier-derived PCAs while accounting for phylogeny. PFDA is derived from flexible discriminant analysis (FDA; Hastie *et al.*, 1994) and corresponds to its phylogenetically informed version (Motani & Schmitz, 2011). PFDA is a classification model based on a combination of linear regressions. It incorporates a phylogenetic distance matrix whose terms are multiplied by lambda (Pagel, 1999). Lambda is optimised to minimise the part of the model error that is due to phylogeny. PFDAs were performed only on the first PC because it yielded

the highest classification rates with the leave-one-out cross-validation procedures. PFDAs were performed with all our 100 phylogenetic trees.

INSTITUTIONAL ABBREVIATIONS

DNM, Natural History Museum of Utah, Salt Lake City, Utah, USA; FMNH, Field Museum of Natural History, Chicago, Illinois, USA; MNHN, Muséum national d'histoire naturelle, Paris, France; MOR, Museum of the Rockies, Bozeman, Montana, USA; RVC, Royal Veterinary College, London, UK; UMZC, Cambridge University Museum of Zoology, Cambridge, UK; YPM, Yale Peabody Museum of Natural History, New Haven, Connecticut, USA.

Results

PHYLOGENETIC SIGNAL IN THE DATA

We uncover a significant phylogenetic signal in body mass (*P*-value between 0.001 and 0.035; mean = 0.001) and P.SD (*P*-value between 0.001 and 0.17; mean = 0.006; Table 2). The K-statistic is always below 1 (from 0.172 to 0.603 and from 0.096 to 0.505, respectively for body mass and P.SD), indicating that closely related species are more different than expected under a Brownian motion evolutionary model and that convergence exists. Locomotion is also significantly associated with the phylogeny (mean *P*-value = 0.001), with the delta-statistic ranging from 8.04 to 376.27 (mean = 22.63). No signal is found in C_{obs}.SD (*P*-value between 0.051 and 0.395; mean = 0.155) and S.SD (*P*-value be-tween 0.097 and 0.654; mean = 0.299).

Table 2. Phylogenetic signal in the data. Values reported in the table are means obtained from 100 phylogenetic trees. Minimum and maximum values are given in parentheses. The *P*-values for delta and K (Blomberg *et al.*, 2003) were obtained from 10 and 1000 randomisations, respectively. Body mass and S.SD were transformed to $\log_{10}$

Parameter	Delta-statistic	K-statistic	*P*-value
Locomotion	22.63 (8.04–376.27)		< 0.001***
Body mass		0.519 (0.172–0.603)	0.001** (0.001–0.035)
C_{obs}.SD		0.167 (0.043–0.232)	0.155 (0.051–0.395)
P.SD		0.37 (0.096–0.505)	0.006** (0.001–0.17)
S.SD		0.145 (0.086–0.205)	0.299 (0.097–0.654)

Asterisks indicate mean *P*-values that are statistically significant: two asterisks (**) indicate a mean *P*-value that is below or equal to 0.01, while three asterisks (***) indicate a mean *P*-value that is below or equal to 0.001.

ANGULAR ANALYSES AND PHYLOMORPHOSPACES

PCA successfully separates the locomotion modes with the parameters C_{obs} and P. Thus, we will focus on the latter in this section. However, the PCA results with the parameter S are available in the Supporting Information (Fig. S1).

For both C_{obs} and P, the number of harmonics aggregating 95% of the harmonic power is 12 (Supporting Information, Fig. S2). For C_{obs}, PCA performs well in segregating bipeds and quadrupeds, primarily along the first PC (Fig. 6A), with the latter accounting for the majority of the variance (90.2%). The first two PCs together account for nearly 95% of the total variance. As shown by the two extreme shapes on either side of the first PC, quadrupeds appear to possess a homogeneous bone compactness in cross-section (left part of the morphological space), whereas bipeds tend to show lower bone compactness anterolaterally and posteromedially (right part of the morphospace). Facultative bipeds are found in the overlap between bipeds and quadrupeds.

Dinosauria (i.e. Theropoda) occupies the right side of the phylomorphospace (Fig. 7A), whereas Crocodylia, Lepidosauria and Testudines are on the left side. Dinosauria and Crocodylia appear to show greater variation along PC2 than Lepidosauria, while Testudines is confined to negative PC values.

For the parameter P, the PCA also achieves good separation between bipeds and quadrupeds, again primarily along the first PC (Fig. 6B), with the latter accounting for the majority of the variance (87.6%). The second PC accounts for 6.12% of the variance. As expected with P, the distribution of locomotor groups in the morphological space is reversed with respect to bone compactness. Bipeds appear to have a homogeneous P in cross-section, as shown by the extreme shape on the left side of the morphological space, whereas quadrupeds tend to show a lower mediolateral P (see the extreme shape on the right of the graph, which is slightly compressed mediolaterally). Facultative bipeds are found in the region of overlap between bipeds and quadrupeds.

Again, the distribution of clades on the phylomorphospace is reversed with respect to bone compactness. Dinosauria occupies the left side of the graph (Fig. 7B), whereas Crocodylia, Lepidosauria and Testudines are on the right side. Dinosauria and Crocodylia show greater variation along PC2 compared to lepidosaurs, while Testudines is restricted to positive PC values (upper right part of the phylomorphospace).

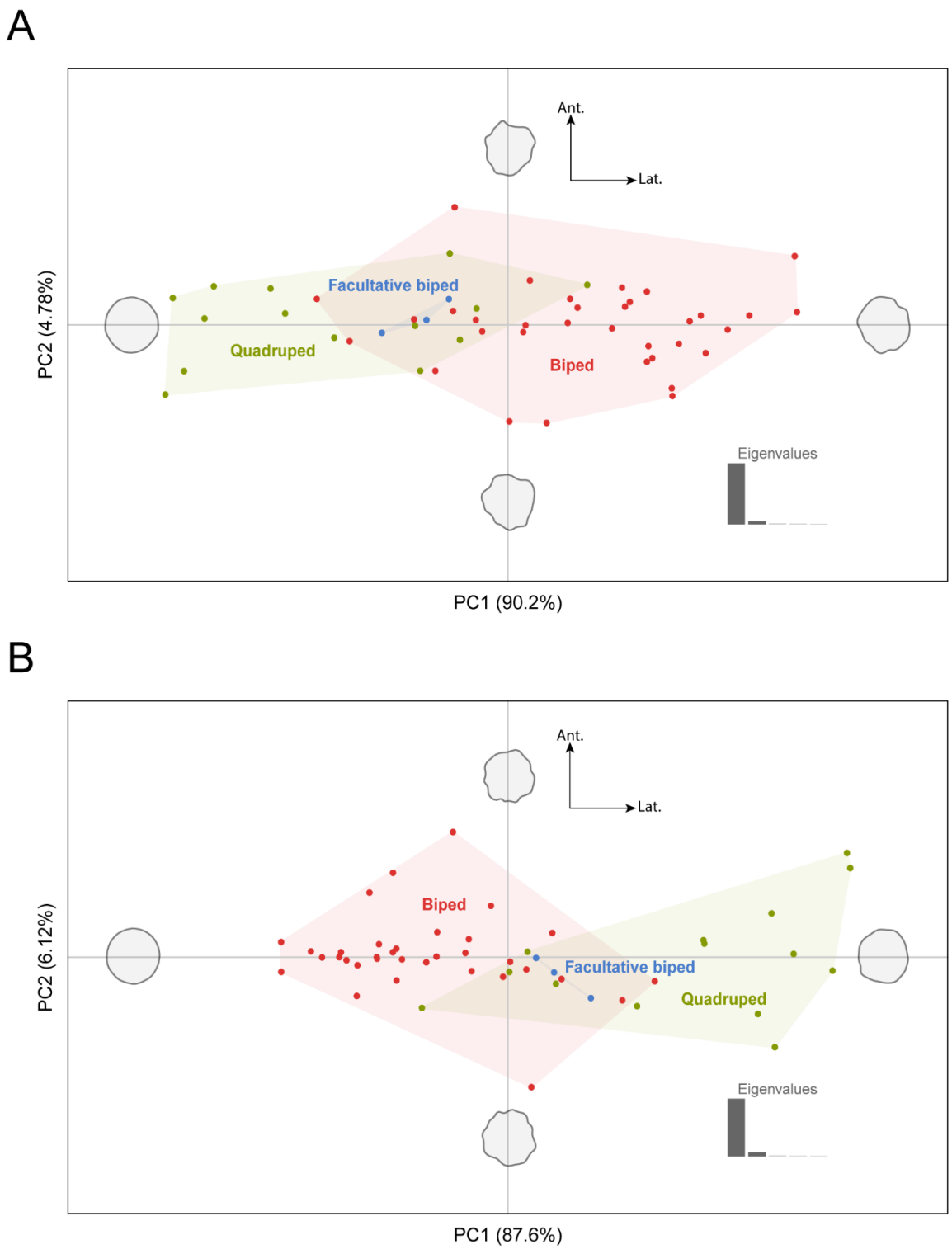

Figure 6. Morphological separation of locomotor modes based on elliptic Fourier coefficients from angular measurements of C_{obs} (A) and P (B), as shown by principal component analysis.

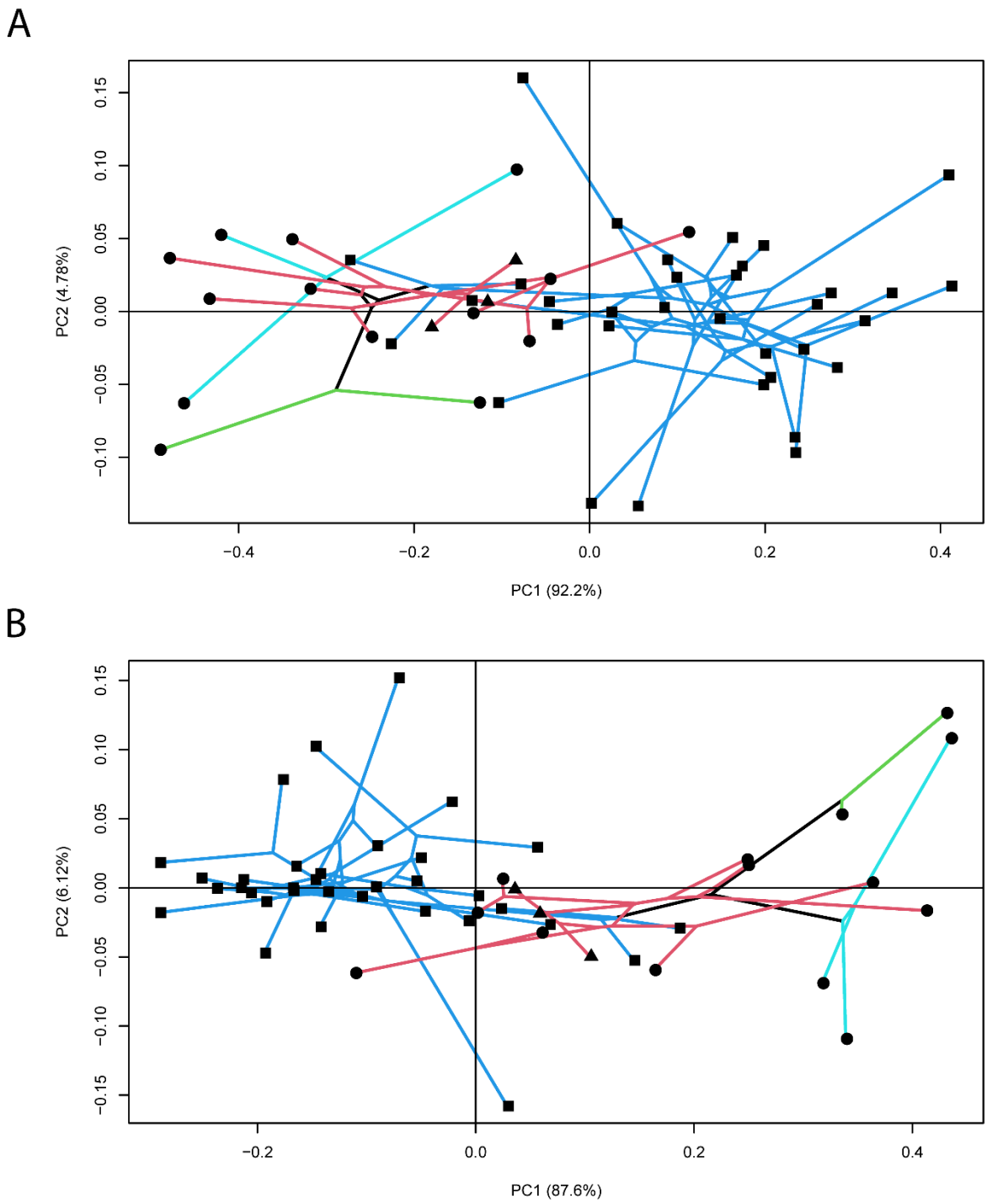

Figure 7. Phylogenetic morphospaces for the microanatomical parameters C_{obs} (A) and P (B) showing the distribution of the major reptilian clades. Blue, Dinosauria; cyan, Crocodylia; green, Testudines; red, Lepidosauria. Circles, quadrupeds; squares, bipeds; triangles, facultative bipeds.

PHYLOGENETIC CLASSIFICATION OF LOCOMOTOR GROUPS

PFDA is moderately successful in discriminating locomotor groups from the first axis of the Fourier-derived PCA for C_{obs} (Fig. 8A). Indeed, the leave-one-out cross-validations for the 100 phylogenetic trees yields a correct classification rate that ranged between 59% and 61% (mean = 60%). On average, bipeds (34) are correctly classified at 52% (50–53%). Quadrupeds (14) are correctly classified at 93% with all tree hypotheses. The three facultative bipeds are never classified correctly. Lambda ranges between 0.48 and 0.58 (mean = 0.529).

PFDA performs slightly better with the parameter P (Fig. 8B). The leave-one-out cross-validation yields a correct classification rate between 63% and 67% (mean = 64%). In-group classification rates are more balanced. Indeed, bipeds are correctly classified at 66% (62–68%) and quadrupeds at 74% (71–79%). Facultative bipeds are never correctly classified. Lambda ranges between 0.4 and 0.48 (mean = 0.442).

RELATIONSHIP BETWEEN BODY MASS AND THE FEMORAL MICROANATOMICAL PARAMETERS

Body mass is significantly associated with P.SD (*P*-value between 0.016 and 0.042; mean = 0.027; Table 3). The lambda parameter ranges from 0.745 to 0.841 (mean = 0.79). However, no association is found with C_{obs}.SD (*P*-value between 0.118 and 0.122; mean = 0.12) and with S.SD (*P*-value between 0.271 and 0.35; mean = 0.304). Furthermore, no association is found between body mass and the coordinates of each taxon on the first PC of the Fourier-derived PCAs (Table 3).

ASSOCIATION OF LOCOMOTION AND FUNCTIONAL ECOLOGY WITH MICROANATOMY

None of the microanatomical parameters are significantly associated with locomotion or functional ecology (Table 4). The taxon coordinates on the first PC of the Fourier-derived PCAs are never significantly associated with locomotion (Table 4). When outliers are removed, i.e., *Allosaurus fragilis*, *Tyrannosaurus rex* and *Iguana iguana* (Linnaeus, 1758), taxon coordinates with the parameters C_{obs} and P become significantly associated with locomotion in 3% and 100% of the tree hypotheses, respectively (see Supporting Information, Table S2). Post-hoc tests reveal that bipeds differ significantly from quadrupeds with the parameter P for 24% of the trees (see Supporting Information, Table S3). The taxon coordinates are never significantly associated with functional ecology (Table 4).

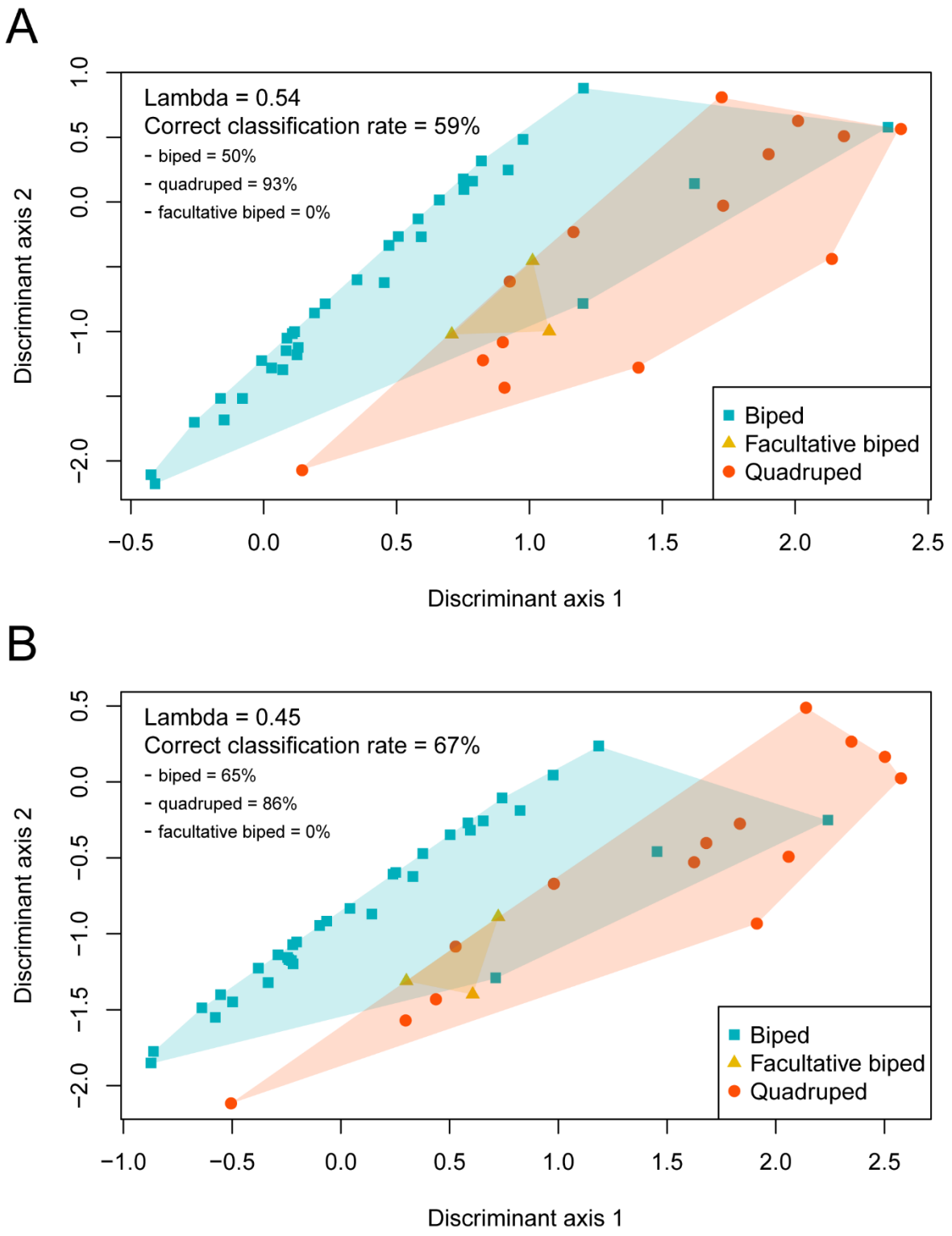

Figure 8. Separation of locomotor categories resulting from phylogenetic flexible discriminant analyses (PFDA) based on the first PC of the Fourier-derived principal component analyses with C_{obs} (A) and P (B).

Table 3. Relationship between body mass and the femoral microanatomical parameters, and the taxon coordinates on PC1 of the Fourier-derived PCAs. Values reported are means obtained from 100 phylogenetic trees. Minimum and maximum values are indicated in parentheses. Body mass and S.SD were $\log_{10}$ transformed

PGLS model formula	R^2	*P*-value	Lambda
C_{obs}.SD ~ Body mass	0.049 (0.048–0.049)	0.120 (0.118–0.122)	< 0.001
P.SD ~ Body mass	0.096 (0.082–0.113)	0.027* (0.016–0.042)	0.790 (0.745–0.841)
S.SD ~ Body mass	0.022 (0.018–0.025)	0.304 (0.271–0.350)	0.133 (0.107–0.183)
PC 1 (C_{obs}) ~ Body mass	0.031 (0.021–0.040)	0.220 (0.162–0.306)	0.781 (0.744–0.820)
PC 1 (P) ~ Body mass	0.024 (0.014–0.033)	0.284 (0.200–0.415)	0.882 (0.852–0.910)

The asterisk (*) indicates a mean *P*-value of less than 0.05.

Table 4. Influence of locomotion and functional ecology on the femoral microanatomical parameters and on the taxon coordinates on PC1 of the Fourier-derived PCAs. Values reported are means obtained from 100 phylogenetic trees. Minimum and maximum values are indicated in parentheses. S.SD was $\log_{10}$ transformed

Phylogenetic ANOVA model formula		F-value	*P*-values
C_{obs}.SD ~	Locomotion	4.645	0.581 (0.533–0.630)
	Functional ecology	1.446	0.830 (0.795–0.867)
P.SD ~	Locomotion	15.702 (15.436–15.997)	0.253 (0.212–0.303)
	Functional ecology	0.905 (0.893–0.918)	0.914 (0.889–0.931)
S.SD ~	Locomotion	4.811	0.574 (0.505–0.623)
	Functional ecology	0.529	0.964 (0.950–0.983)
PC 1 (C_{obs}) ~	Locomotion	22.680	0.165 (0.129–0.200)
	Functional ecology	0.690	0.945 (0.920–0.971)
PC 1 (P) ~	Locomotion	31.552	0.101 (0.064–0.129)
	Functional ecology	0.691	0.944 (0.928–0.967)

Discussion

NATURE OF THE DATA AND EFFECT OF PHYLOGENETIC, ALLOMETRIC, ENVIRONMENTAL AND FUNCTIONAL FACTORS

Locomotion, body mass and the P.SD parameter carry a phylogenetic signal. In the case of body mass and P.SD, the K statistic is less than 1 and suggests convergence. The presence of a phylogenetic signal, at least in some parameters, justifies the use of comparative phylogenetic methods.

P.SD is the only microanatomical parameter to be significantly associated with body mass and none of the parameters seem to be associated with functional ecology or locomotion, which may seem surprising at first glance given that PCA manages to correctly separate locomotor modes, at least for the parameters C_{obs} and P. Indeed, C_{obs}.SD, P.SD and S.SD, and the 60 angular values of C_{obs}, P and S do not convey the same information: C_{obs}.SD, P.SD and S.SD correspond to measures of standard deviation, whereas the 60 angular values of C_{obs}, P and S, considered as a whole in the context of Fourier analyses, contain shape information. Therefore, at least in this case, it is important not to consider these two types of metrics as equivalent.

MORPHOMETRIC SEPARATION OF LOCOMOTOR GROUPS

PCA on Fourier coefficients correctly separates the locomotor modes, at least for the parameters C_{obs} and P (Fig. 6). Along PC1, C_{obs} tends to be homogeneous in quadrupeds, whereas bipeds show lower compactness in anterolateral and posteromedial positions. Conversely, quadrupeds have a lower mediolateral P, whereas bipeds have a relatively homogeneous P. This apparent lack of correlation between C_{obs} and P is surprising because they generally evolve in an inverse fashion: if C_{obs} increases, P decreases and reciprocally (Castanet & Caetano, 1995; Canoville & Laurin, 2009). This may be related to the presence of more or less spongiosa. For example, a mediolateral development of cancellous bone into the medullary cavity could account for constant compactness and lower P in this direction in quadrupeds. Although this is correct in theory, examination of the specimens revealed that the vast majority were devoid of spongiosa. Hence, this lack of correlation clearly is artificial. The apparent homogeneity of C_{obs} and P for quadrupeds and bipeds, respectively, comes from the fact that in these two cases the measured values vary while being close to 1. To clarify, for the same amplitude of variation, it tends to be less visible on the shapes reconstructed with the efourier function when the values of the microanatomical parameter considered are high than when they are close to 0. By observing the raw data, it is clear that high values of C_{obs} correspond to low values of P for a given taxon, and vice versa. This is even more evident when looking at the PCA plots (Fig. 6): we notice a mirror effect between C_{obs} and P. The inverse relationship between C_{obs} and P is thus confirmed, which implies that when studying the medullocortical transition, considering only one of these parameters is sufficient and prevents redundancies.

Now, does this variation in compactness correspond to real variations in the thickness of the cortex? At first sight, this is not obvious (see Fig. 1). Another explanation lies in the eccentricity (an off-centred medullary region) of the cross-sections. If a cross-section shows

eccentricity, bone compactness, as measured with BoneProfileR, will be lower where the cortex is furthest from the centre, even if the cortical thickness is constant. The majority of the cross-sections considered do present eccentricity (see Supporting Information, Table S4) and the direction of elongation tends to be in line with the PCA results for quadrupeds and bipeds: quadrupeds present anteroposterior eccentricity and bipeds anterolateral-posteromedial eccentricity.

These differences can be explained by the biomechanical constraints experienced by the femur. The sampled quadrupeds show a strong abduction of the femur (sprawling and 'semi-erect' taxa represented by lepidosaurs and turtles, and crocodylians, respectively), unlike the sampled bipeds ('crouched' and erect taxa represented by avian and non-avian theropods). In the former, the anterior aspect of the femur, as defined in this study, is dorsally oriented, whereas in the latter, the anterior aspect is craniolaterally oriented. Wilson & Carrano (1999) associated the strong eccentricity observed in the femora of sauropod dinosaurs with a 'wide-gauged' stance, with the feet spread out from the midline. The compressive forces due to weight are accompanied by a lateral component directed from the centre of mass located near the pelvis towards the limbs, which results in mediolateral eccentricity. A wide-gauged stance increases this lateral transmission and thus the eccentricity. Maidment *et al.* (2012) also suggested that because some ornithopod dinosaurs placed their feet directly under the body during locomotion, the vertical ground reaction force combined with the slightly flexed hind limb incurred stresses that predominantly were directed craniocaudally, resulting in eccentricity of bone shape in that direction. In a sense, sprawling to 'semi-erect' taxa can be considered to have a 'very wide gauge' stance, implying greater lateral transmission of forces between the pelvis and femoral shaft, resulting in a bending moment (Blob & Biewener, 1999, 2001) that may account for the dorsoventral eccentricity observed in the quadrupeds in our sample. In the birds and other theropod dinosaurs in our sample, the eccentricity is craniolateral although they moved with their feet close to the midline. A plausible biomechanical explanation for this phenomenon could be that in birds and other theropods, the femur is oriented slightly laterally (abducted), which could induce an additional lateral transmission of forces (= laterally oriented bending stresses) resulting in a craniolateral eccentricity, even though they place their feet under their body (e.g. Hutchinson & Gatesy, 2000).

PHYLOGENY VS. LOCOMOTION

Based on the projection of the phylogeny onto the morphological space of the PCAs, the observations are mostly grouped by clade, with birds on one side of the graph, and lepidosaurs,

turtles and crocodylians on the other (Fig. 7). This is far from surprising since all bipeds are contained in a single clade (birds/Theropoda). We are actually constrained by our taxonomic sampling. In this context, it is difficult to assert with certainty the existence of a functional signal that would not be solely due to phylogeny. However, correct classification rates of about 60–70% from PFDAs and significant phylogenetic ANOVAs (see Supporting Information, Table S2) suggest that despite a phylogenetic effect, the data appear to contain a substantial functional signal. Furthermore, we provide biomechanical arguments that are fully congruent with the microanatomical patterns we observe (see above).

Conclusion

We show that the parameter P.SD is the only microanatomical parameter to carry a phylogenetic signal and to be significantly associated with body mass. The parameters C_{obs}.SD and S.SD are not related to phylogeny, body mass nor functional ecology. This seems contradictory at first sight, as Fourier-derived PCAs are able to separate the locomotor modes. This is most likely due to the nature of the parameters themselves. Indeed, C_{obs}.SD, P.SD and S. are, in fact, not microanatomical parameters but statistical values corresponding to the standard deviations of C_{obs}, P and S, whereas the latter reflect shapes in the context of Fourier analyses.

PCAs performed on the Fourier coefficients properly separate the modes of locomotion for the parameters C_{obs} and P (the angular distributions of bone compactness and the distance of the medullocortical transition from the centre of a cross-section, respectively), mainly along the first component which explains most of the variation (about 90%). Bone compactness is lower in the anterolateral-posteromedial position in bipeds and in the mediolateral position in quadrupeds. The apparent non-correlation between C_{obs} and P actually is artificial, as it is due to high values of C_{obs} and P in quadrupeds and bipeds, respectively. The results with C_{obs} and P basically are redundant. This implies that only one of these two parameters is necessary to study the medullocortical transition in this context.

This differential variation in bone compactness between bipeds and quadrupeds is consistent with the anterolateral-posteromedial and anteroposterior cross-sectional eccentricity in bipeds and quadrupeds, respectively. In both cases, the eccentricity of the cross-section is most likely determined by the posture adopted by the two locomotor modes. The bipeds in our sample have an erect or crouched posture with the anterior surface of the femur facing forward and with low femoral abduction (birds), whereas the quadrupeds have a sprawling or ‘semi-erect’ posture with the anterior surface of the femur facing more dorsally, combined with high

femoral abduction (lepidosaurs and crocodylians). Hence, the lateral transmission of forces related to weight from the centre of mass to the ground could explain the eccentricity observed in the taxa of our sample.

Finally, phylogeny clearly seems to impact our results, as shown by the phylomorphospaces. Nevertheless, correct classification rates over 60% from some PFDAs and significant phylogenetic ANOVAs, sustained by cogent biomechanical arguments, still suggest the presence of a substantial functional signal in the data.

This study shows the impact of locomotion on the shape of mid-diaphyseal femur cross-sections among Reptilia. Using statistical methods that take phylogeny into account, this study provides a better understanding of the locomotor diversity in this clade. The addition of new taxa, including facultative bipeds, but also taxa with a more developed spongiosa, would improve our understanding of the complex interaction between locomotion, femoral cross-sectional geometry and phylogeny in reptiles. The results of this study could ultimately be useful in palaeontology, especially in species for which locomotion remains uncertain. Indeed, in an actualistic context, the acquisition of prior knowledge on extant taxa (bipedal/ quadrupedal) is an essential tool to address past locomotor diversity.

Acknowledgments

We warmly thank Alexandra Houssaye, Margot Michaud and Laura Bento Da Costa for their valuable advice and Mathilde Aladini for her kind review of the manuscript. We are indebted to Peter J. Bishop and Andrew A. Farke for sharing with us the CT data of some of the studied specimens. We are grateful to Renaud Lebrun and the Montpellier ressources imagerie (MRI) platform of the Université de Montpellier as well as Marta Bellato and the Accès scientifique à la tomographie à rayons X (AST-RX) platform of the MNHN for their help in collecting CT data. We thank the anonymous referees and the editors, Nick Fraser and Maarten Christenhusz, whose comments helped to improve the quality of this study. We also thank the Natural History Museum of Utah (UMNH) and the Museum of the Rockies (MOR) for permission to use CT data from their collections. The authors acknowledge the support of the Virtual Data initiative, run by the Laboratoire d'excellence Physique des deux infinis et des origines (LabEX P2IO) and supported by Université Paris-Saclay, for providing computing resources on its cloud infrastructure. This work was supported by the doctoral programme Interfaces pour le vivant (IPV) with Sorbonne Université and by the European Research Council (ERC) under the

European Union's Horizon 2020 research and innovation programme (grant no. 695517 to J.R.H].

Conflict of interest

The authors declare that they have no conflicts of interest.

References

Abràmoff MD, **Magalhães PJ**, **Ram SJ. 2004**. Image processing with ImageJ. *Biophotonics International* **11**: 36–42.

Amson E, **Kolb C. 2016**. Scaling effect on the mid-diaphysis properties of long bones—the case of the Cervidae (deer). *The Science of Nature* **103**: 58.

Amson E, **de Muizon C**, **Laurin M**, **Argot C**, **de Buffrénil V. 2014**. Gradual adaptation of bone structure to aquatic lifestyle in extinct sloths from Peru. *Proceedings of the Royal Society B: Biological Sciences* **281**: 20140192.

Bakker RT, **Galton PM. 1974**. Dinosaur monophyly and a new class of vertebrates. *Nature* **248**: 168–172.

Bapst DW, **Wright AM**, **Matzke NJ**, **Lloyd GT. 2016**. Topology, divergence dates, and macroevolutionary inferences vary between different tip-dating approaches applied to fossil theropods (Dinosauria). *Biology Letters* **12**: 1–4.

Bels V, **Russell AP. 2019**. *Behavior of lizards: evolutionary and mechanistic perspectives*. Boca Raton: CRC Press.

Bennett G. 1875. Notes on the *Chlamydosaurus* or frilled lizard of Queensland (*Chlamydosaurus kingii*, Gray), and the discovery of a fossil species on the Darling Downs, Queensland. *Papers and Proceedings of the Royal Society of Tasmania* **1875**: 56–58.

Benton MJ, **Dhouailly D**, **Jiang B**, **McNamara M. 2019**. The early origin of feathers. *Trends in Ecology & Evolution* **34**: 856–869.

Bishop PJ, **Hocknull SA**, **Clemente CJ**, **Hutchinson JR**, **Barrett RS**, **Lloyd DG. 2018a**. Cancellous bone and theropod dinosaur locomotion. Part II—a new approach to inferring posture and locomotor biomechanics in extinct tetrapod vertebrates. *PeerJ* **6**: e5779.

Bishop PJ, **Hocknull SA**, **Clemente CJ**, **Hutchinson JR**, **Farke AA**, **Barrett RS**, **Lloyd DG. 2018b**. Cancellous bone and theropod dinosaur locomotion. Part III—inferring posture and locomotor biomechanics in extinct theropods, and its evolution on the line to birds. *PeerJ* **6**: e5777.

Bishop PJ, **Hocknull SA**, **Clemente CJ**, **Hutchinson JR**, **Farke AA**, **Beck BR**, **Barrett RS**, **Lloyd DG. 2018c**. Cancellous bone and theropod dinosaur locomotion. Part I—an examination of cancellous bone architecture in the hindlimb bones of theropods. *PeerJ* **6**: e5778.

Blob RW, **Biewener AA. 1999**. *In vivo* locomotor strain in the hindlimb bones of *Alligator mississippiensis* and *Iguana iguana*: implications for the evolution of limb bone safety factor and non-sprawling limb posture. *Journal of Experimental Biology* **202**: 1023–1046.

Blob RW, **Biewener AA. 2001**. Mechanics of limb bone loading during terrestrial locomotion in the green iguana (*Iguana iguana*) and American alligator (*Alligator mississippiensis*). *Journal of Experimental Biology* **204**: 1099–1122.

Blomberg SP, **Garland T**, **Ives AR. 2003**. Testing for phylogenetic signal in comparative data: behavioral traits are more labile. *Evolution* **57**: 717–745.

Bonhomme V, **Picq S**, **Gaucherel C**, **Claude J. 2014**. Momocs: outline analysis using R. *Journal of Statistical Software* **56**: 1–24.

Bonhomme V, **Prasad S**, **Gaucherel C. 2013**. Intraspecific variability of pollen morphology as revealed by elliptic Fourier analysis. *Plant Systematics and Evolution* **299**: 811–816.

Borges R, **Machado JP**, **Gomes C**, **Rocha AP**, **Antunes A. 2019**. Measuring phylogenetic signal between categorical traits and phylogenies. *Bioinformatics* **35**: 1862–1869.

Brett-Surman MK, Holtz TR, Farlow JO, eds. 2012. *The complete dinosaur*. Bloomington: Indiana University Press.

Cadet F, **Fontaine N**, **Vetrivel I**, **Ng Fuk Chong M**, **Savriama O**, **Cadet X**, **Charton P. 2018**. Application of Fourier transform and proteochemometrics principles to protein engineering. *BMC Bioinformatics* **19**: 1–11.

Caillon F, **Bonhomme V**, **Möllmann C**, **Frelat R. 2018**. A morphometric dive into fish diversity. *Ecosphere* **9**: e02220.

Campione NE. 2020. *MASSTIMATE: body mass estimation equations for vertebrates*. R package version 2.0-1. https://CRAN.R-project.org/package=MASSTIMATE

Campione NE, **Evans DC. 2012**. A universal scaling relationship between body mass and proximal limb bone dimensions in quadrupedal terrestrial tetrapods. *BMC Biology* **10**: 1–22.

Campione NE, **Evans DC**, **Brown CM**, **Carrano MT. 2014**. Body mass estimation in non-avian bipeds using a theoretical conversion to quadruped stylopodial proportions. *Methods in Ecology and Evolution* **5**: 913–923.

Canoville A, **Laurin M. 2009**. Microanatomical diversity of the humerus and lifestyle in lissamphibians. *Acta Zoologica* **90**: 110–122.

Canoville A, **Laurin M. 2010**. Evolution of humeral microanatomy and lifestyle in amniotes, and some comments on palaeobiological inferences. *Biological Journal of the Linnean Society* **100**: 384–406.

Castanet J, **Caetano MH. 1995**. Influence du mode de vie sur les caractéristiques pondérales et structurales du squelette chez les amphibiens anoures. *Canadian Journal of Zoology* **73**: 234–242.

Chiari Y, **Cahais V**, **Galtier N**, **Delsuc F. 2012**. Phylogenomic analyses support the position of turtles as the sister group of birds and crocodiles (Archosauria). *BMC Biology* **10**: 1–15.

Clemente CJ, **Wu NC. 2018**. Body and tail-assisted pitch control facilitates bipedal locomotion in Australian agamid lizards. *Journal of the Royal Society Interface* **15**: 20180276.

Cooper LN, **Clementz MT**, **Usip S**, **Bajpai S**, **Hussain ST**, **Hieronymus TL. 2016**. Aquatic habits of cetacean ancestors: integrating bone microanatomy and stable isotopes. *Integrative and Comparative Biology* **56**: 1370–1384.

Currey JD. 2013. *Bones: structure and mechanics*. Princeton: Princeton University Press.

Dawson JW. 1860. On a terrestrial mollusk, a chilognathous myriapod, and some new species of reptiles, from the coal- formation of Nova Scotia. *Quarterly Journal of the Geological Society* **16**: 268–277.

Demes B. 2011. Three-dimensional kinematics of capuchin monkey bipedalism. *American Journal of Physical Anthropology* **145**: 147–155.

Didier G, **Laurin M. 2020**. Exact distribution of divergence times from fossil ages and tree topologies. *Systematic Biology* **69**: 1068–1087.

Dodson P. 2000. Origin of birds: the final solution? *American Zoologist* **40**: 504–512.

Doube M, **Klosowski MM**, **Arganda-Carreras I** , **Cordelières FP**, **Dougherty RP**, **Jackson JS**, **Schmid B**, **Hutchinson JR**, **Shefelbine SJ. 2010**. BoneJ: free and extensible bone image analysis in ImageJ. *Bone* **47**: 1076–1079.

Drumheller SK, **Wilberg EW. 2020**. A synthetic approach for assessing the interplay of form and function in the crocodyliform snout. *Zoological Journal of the Linnean Society* **188**: 507–521.

Duméril AHA. 1856. Description des reptiles nouveaux ou imparfaitement connus de la collection du Muséum d'Histoire Naturelle et remarques sur la classification et les caractères des reptiles. *Archives du Muséum d'Histoire Naturelle* **8**: 438–588.

Dumont M, **Laurin M**, **Jacques F**, **Pellé E**, **Dabin W**, **de Buffrénil V. 2013**. Inner architecture of vertebral centra in terrestrial and aquatic mammals: a two-dimensional comparative study. *Journal of Morphology* **274**: 570–584.

Fabbri M, **Navalón G**, **Benson RBJ**, **Pol D**, **O'Connor J**, **Bhullar BAS**, **Erickson GM**, **Norell MA**, **Orkney A**, **Lamanna MC**, **Zouhri S**, **Becker J**, **Emke A**, **Dal Sasso C**, **Bindellini G**, **Maganuco S**, **Auditore M**, **Ibrahim N. 2022**. Subaqueous foraging among carnivorous dinosaurs. *Nature* **603**: 8521–8857.

Felsenstein J. 1985. Phylogenies and the comparative method. *The American Naturalist* **125**: 1–15.

Fürbringer M. 1888. *Untersuchungen zur Morphologie und Systematik der Vögel: zugleich ein Beitrag zur Anatomie der Stütz-und Bewegungsorgane*. Amsterdam: T. van Holkema.

Garland T, **Dickerman AW**, **Janis CM**, **Jones JA. 1993**. Phylogenetic analysis of covariance by computer simulation. *Systematic Biology* **42**: 265–292.

Gatesy SM. 1991. Hind limb movements of the American alligator (*Alligator mississippiensis*) and postural grades. *Journal of Zoology* **224**: 577–588.

Germain D, **Laurin M. 2005**. Microanatomy of the radius and lifestyle in amniotes (Vertebrata, Tetrapoda). *Zoologica Scripta* **34**: 335–350.

Girondot M, **Laurin M. 2003**. Bone Profiler: a tool to quantify, model, and statistically compare bone-section compactness profiles. *Journal of Vertebrate Paleontology* **23**: 458–461.

Gmelin JF. 1789. *Systema naturae per regna tria naturae, secundum classes, ordines, genera, species, cum characteribus, differentiis, synonymis, locis*. Leipzig: G.E. Beer.

Gônet J, **Laurin M**, **Girondot M. 2022**. BoneProfileR: the next step to quantify, model and statistically compare bone section compactness profiles. *Palaeontologia Electronica* **25**: a12.

Gray J. 1825. A synopsis of the genera of reptiles and Amphibia, with a description of some new species. *Annals of Philosophy* **10**: 193–217.

Gray JE. 1838. Catalogue of the slender-tongued saurians, with descriptions of many new genera and species. Part 3. *Journal of Natural History* **1**: 388–394.

Grigg G, **Kirshner D. 2015**. *Biology and evolution of crocodylians*. Clayton: CSIRO Publishing.

Grinham LR, **Norman DB. 2020**. The pelvis as an anatomical indicator for facultative bipedality and substrate use in lepidosaurs. *Biological Journal of the Linnean Society* **129**: 398–413.

Hastie T, **Tibshirani R**, **Buja A. 1994**. Flexible discriminant analysis by optimal scoring. *Journal of the American Statistical Association* **89**: 1255–1270.

Houssaye A, **Botton-Divet L. 2018**. From land to water: evolutionary changes in long bone microanatomy of otters (Mammalia: Mustelidae). *Biological Journal of the Linnean Society* **125**: 240–249.

Houssaye A, **Sander PM**, **Klein N. 2016a**. Adaptive patterns in aquatic amniote bone microanatomy—more complex than previously thought. *Integrative and Comparative Biology* **56**: 1349–1369.

Houssaye A, **Taverne M**, **Cornette R. 2018**. 3D quantitative comparative analysis of long bone diaphysis variations in microanatomy and cross-sectional geometry. *Journal of Anatomy* **232**: 836–849.

Houssaye A, **Waskow K**, **Hayashi S**, **Cornette R**, **Lee AH**, **Hutchinson JR. 2016b**. Biomechanical evolution of solid bones in large animals: a microanatomical investigation. *Biological Journal of the Linnean Society* **117**: 350–371.

Hutchinson JR, **Bates KT**, **Molnar JL**, **Allen V**, **Makovicky PJ. 2011**. A computational analysis of limb and body dimensions in *Tyrannosaurus rex* with implications for locomotion, ontogeny, and growth. *PLoS One* **6**: e26037.

Hutchinson JR, **Gatesy SM. 2000**. Adductors, abductors, and the evolution of archosaur locomotion. *Paleobiology* **26**: 734–751.

Hutchinson JR, **Gatesy SM. 2001**. Bipedalism. In: *Encyclopedia of Life Sciences*. Hoboken: Wiley, 1–6.

Huxley TH. 1868. On the animals which are most nearly intermediate between birds and reptiles. *Annals and Magazine of Natural History* **2**: 66–75.

Ibrahim N, **Sereno PC**, **Dal Sasso C**, **Maganuco S**, **Fabbri M**, **Martill DM**, **Zouhri S**, **Myhrvold NP**, **Iurino DA. 2014**. Semiaquatic adaptations in a giant predatory dinosaur. *Science* **345**: 1613–1616.

Jetz W, **Thomas GH**, **Joy JB**, **Hartmann K**, **Mooers AO. 2012**. The global diversity of birds in space and time. *Nature* **491**: 444–448.

Joyce WG, **Parham JF**, **Lyson TR**, **Warnock RCM**, **Donoghue PCJ. 2013**. A divergence dating analysis of turtles using fossil calibrations: an example of best practices. *Journal of Paleontology* **87**: 612–634.

Klein N, **Sander PM**, **Krahl A**, **Scheyer TM**, **Houssaye A. 2016**. Diverse aquatic adaptations in *Nothosaurus* spp. (Sauropterygia)—inferences from humeral histology and microanatomy. *PLoS One* **11**: e0158448.

Kriloff A, **Germain D**, **Canoville A**, **Vincent P**, **Sache M**, **Laurin M. 2008**. Evolution of bone microanatomy of the tetrapod tibia and its use in palaeobiological inference. *Journal of Evolutionary Biology* **21**: 807–826.

Kruta I, **Bardin J**, **Smith CP**, **Tafforeau P**, **Landman NH. 2020**. Enigmatic hook-like structures in Cretaceous ammonites (Scaphitidae). *Palaeontology* **63**: 301–312.

Kuhl FP, **Giardina CR. 1982**. Elliptic Fourier features of a closed contour. *Computer Graphics and Image Processing* **18**: 236–258.

Laurin M, **Canoville A**, **Germain D. 2011**. Bone microanatomy and lifestyle: a descriptive approach. *Comptes Rendus Palevol* **10**: 381–402.

Lebrun R. 2018. MorphoDig, an open-source 3D freeware dedicated to biology. 5th International Palaeontological Congress.

Linnaeus C. 1758. *Systema naturae per regna tria naturae, secundum classes, ordines, genera, species, cum characteribus, differentiis, synonymis, locis*. Stockholm: L. Salvius.

Lovette IJ, **Fitzpatrick JW. 2016**. *Handbook of bird biology*. Hoboken: Wiley.

Maidment SCR, **Linton DH**, **Upchurch P**, **Barrett PM. 2012**. Limb-bone scaling indicates diverse stance and gait in quadrupedal ornithischian dinosaurs. *PLoS One* **7**: e36904.

Marsh OC. 1877. Notice of new dinosaurian reptiles from the Jurassic formation. *American Journal of Science and Arts* **14**: 514–516.

Martins EP, **Hansen TF. 1997**. Phylogenies and the comparative method: a general approach to incorporating phylogenetic information into the analysis of interspecific data. *The American Naturalist* **149**: 646–667.

von Meyer H. 1861. *Archaeopteryx lithographica* (Vogel-Feder) und *Pterodactylus* von Solnhofen. *Neues Jahrbuch für Mineralogie, Geognosie, Geologie und Petrefaktenkunde* **1861**: 678–679.

Motani R, **Schmitz L. 2011**. Phylogenetic versus functional signals in the evolution of form-function relationships in terrestrial vision. *Evolution* **65**: 2245–2257.

Myhrvold NP, **Baldridge E**, **Chan B**, **Sivam D**, **Freeman DL**, **Ernest SKM. 2015**. An amniote life-history database to perform comparative analyses with birds, mammals, and reptiles. *Ecology* **96**: 3109.

Nakajima Y, **Hirayama R**, **Endo H. 2014**. Turtle humeral microanatomy and its relationship to lifestyle. *Biological Journal of the Linnean Society* **112**: 719–734.

Nyakatura JA, **Melo K**, **Horvat T**, **Karakasiliotis K**, **Allen VR**, **Andikfar A**, **Andrada E**, **Arnold P**, **Lauströer J**, **Hutchinson JR**, **Fischer MS**, **Ijspeert AJ. 2019**. Reverse-engineering the locomotion of a stem amniote. *Nature* **565**: 351–355.

Orme D, **Freckleton R**, **Thomas G**, **Petzoldt T**, **Fritz S**, **Isaac N**, **Pearse W. 2018**. *The caper package: comparative analysis of phylogenetics and evolution in R*. R package version 1.0.1. https://CRAN.R-project.org/package=caper.

Osborn HF. 1905. *Tyrannosaurus* and other Cretaceous carnivorous dinosaurs. *Bulletin of the American Museum of Natural History* **21**: 259–265.

Ostrom JH. 1969. Osteology of *Deinonychus antirrhopus*, an unusual theropod from the Lower Cretaceous of Montana. *Bulletin of the Yale Peabody Museum of Natural History* **30**: 1–165.

Ostrom JH. 1975. The origin of birds. *Annual Review of Earth and Planetary Sciences* **3**: 55–77.

Owen R. 1843. On *Dinornis novæ-zealandiæ*. *Proceedings of the Zoological Society of London* **11**: 8–10.

Padian K, **Chiappe LM. 1998**. The origin and early evolution of birds. *Biological Reviews* **73**: 1–42.

Pagel M. 1999. Inferring the historical patterns of biological evolution. *Nature* **401**: 877–884.

Persons WS, **Currie PJ**, **Erickson GM. 2020**. An older and exceptionally large adult specimen of *Tyrannosaurus rex*. *Anatomical Record* **303**: 656–672.

Pianka ER, **Vitt LJ. 2003**. *Lizards: windows to the evolution of diversity*. Berkeley: University of California Press.

Plasse M, **Amson E**, **Bardin J**, **Grimal Q**, **Germain D. 2019**. Trabecular architecture in the humeral metaphyses of non-avian reptiles (Crocodylia, Squamata and Testudines): lifestyle, allometry and phylogeny. *Journal of Morphology* **280**: 982–998.

Quemeneur S, **de Buffrénil V**, **Laurin M. 2013**. Microanatomy of the amniote femur and inference of lifestyle in limbed vertebrates. *Biological Journal of the Linnean Society* **109**: 644–655.

R Core Team. 2013. *R: a language and environment for statistical computing.* Vienna: R Foundation for Statistical Computing.

Ransom SM, **Eikenberry SS**, **Middleditch J. 2002**. Fourier techniques for very long astrophysical time-series analysis. *Astronomical Journal* **124**: 1788–1809.

Rauhut OWM, **Pol D. 2019**. Probable basal allosauroid from the early Middle Jurassic Cañadón Asfalto Formation of Argentina highlights phylogenetic uncertainty in tetanuran theropod dinosaurs. *Scientific Reports* **9**: 18826.

Reilly SM, **Elias JA. 1998**. Locomotion in *Alligator mississippiensis*: kinematic effects of speed and posture and their relevance to the sprawling-to-erect paradigm. *Journal of Experimental Biology* **201**: 2559–2574.

Revell LJ. 2012. Phytools: an R package for phylogenetic comparative biology (and other things). *Methods in Ecology and Evolution* **3**: 217–223.

Robling AG, **Castillo AB**, **Turner CH. 2006**. Biomechanical and molecular regulation of bone remodeling. *Annual Review of Biomedical Engineering* **8**: 455–498.

Rygel M, Lally C, Gibling M, Ielpi A, Calder J, Bashforth A. 2015. Sedimentology and stratigraphy of the type section of the Pennsylvanian Boss Point Formation, Joggins Fossil Cliffs, Nova Scotia, Canada. *Atlantic Geology* **51**: 1–43.

Sampson SD, **Carrano MT**, **Forster CA. 2001**. A bizarre predatory dinosaur from the Late Cretaceous of Madagascar. *Nature* **409**: 504–506.

Schuett GW, **Reiserer RS**, **Earley RL. 2009**. The evolution of bipedal postures in varanoid lizards. *Biological Journal of the Linnean Society* **97**: 652–663.

Sereno PC. 1997. The origin and evolution of dinosaurs. *Annual Review of Earth and Planetary Sciences* **25**: 435–489.

Shapiro B, **Sibthorpe D**, **Rambaut A**, **Austin J**, **Wragg GM**, **Bininda-Emonds ORP**, **Lee PLM**, **Cooper A. 2002**. Flight of the dodo. *Science* **295**: 1683–1683.

Simpson GG. 1946. Fossil penguins. *Bulletin of the American Museum of Natural History* **87**: 1–95.

Snyder RC. 1949. Bipedal locomotion of the lizard *Basiliscus basiliscus*. *Copeia* **1949**: 129–137.

Sues HD. 2019. *The rise of reptiles: 320 million years of evolution*. Baltimore: John Hopkins University Press.

Symonds MRE, **Blomberg SP. 2014**. A primer on phylogenetic generalised least squares. In: Garamszegi LZ, ed. *Modern phylogenetic comparative methods and their application in evolutionary biology*. Berlin: Springer, 105–130.

Tonini JFR, **Beard KH**, **Ferreira RB**, **Jetz W**, **Pyron RA. 2016**. Fully-sampled phylogenies of squamates reveal evolutionary patterns in threat status. *Biological Conservation* **204**: 23–31.

Turner AH, **Pritchard AC**, **Matzke NJ. 2017**. Empirical and Bayesian approaches to fossil-only divergence times: a study across three reptile clades. *PLoS One* **12**: e0169885.

Utting J, **Giles PS**, **Dolby G. 2010**. Palynostratigraphy of Mississippian and Pennsylvanian rocks, Joggins area, Nova Scotia and New Brunswick, Canada. *Palynology* **34**: 43–89.

Wagstaffe AY, **O'Driscoll AM**, **Kunz CJ**, **Rayfield EJ**, **Janis CM. 2022**. Divergent locomotor evolution in 'giant' kangaroos: evidence from foot bone bending resistances and microanatomy. *Journal of Morphology* **283**: 313–332.

Wilson JA, **Carrano MT. 1999**. Titanosaurs and the origin of 'wide-gauge' trackways: a biomechanical and systematic perspective on sauropod locomotion. *Paleobiology* **25**: 252–267.

Wyneken J, **Godfrey MH**, **Bels V. 2007**. *Biology of turtles: from structures to strategies of life*. Boca Raton: CRC Press.

Zaharias P, **Kantor YI**, **Fedosov AE**, **Criscione F**, **Hallan A**, **Kano Y**, **Bardin J**, **Puillandre N. 2020**. Just the once will not hurt: DNA suggests species lumping over two oceans in deep-sea snails (Cryptogemma). *Zoological Journal of the Linnean Society* **190**: 532–557.

Supporting information

Additional supporting information may be found in the online version of this article on the publisher's website.